

Spatial coherence of thermal photons favors photosynthetic life

Pedro Manrique¹, Adriana De Mendoza², Felipe Caycedo-Soler³, Ferney Rodríguez²,
Luis Quiroga², Neil Johnson¹

July 29, 2022

1. Physics Department, University of Miami, Coral Gables, Florida FL 33126, U.S.A.
2. Departamento de Física, Universidad de Los Andes, A.A. 4976, Bogotá, Colombia
3. Institute of Theoretical Physics, University of Ulm, Albert-Einstein-Allee 11, D - 89069 Ulm, Germany

Abstract

Harvesting of sunlight underpins Life on Earth as well as driving novel energy device design [1, 2, 3, 4, 5]. Though several experiments suggest that excitation energy transport and charge separation within a photosynthetic membrane may benefit from the quantum nature of their dynamics [2, 6, 7, 8], the effects of spatial coherences in the incident light have been largely ignored. Here we show that spatial correlations in the incident light likely play an important role in trapping light and adding robustness, as well as providing a driving mechanism for an organism's adaptation toward more ordered structures. Our theory is grounded by empirical inputs, while its output is validated against testable predictions. Our results suggest that spatiotemporal correlations between photons, a fundamental property of the quantum world, should play a key role in our understanding of early Life and in improving the design of artificial photosynthetic systems.

The nature and possible uses of the quantum-mechanical correlations within light continue to generate heated debates. While the photoelectric effect establishes that light transfers energy to materials through the capture of individual energy packets (photons), experiments probing Bell inequalities and Hanbury-Brown-

Twiss effects show that photons can also exhibit highly non-trivial spatial correlations – even within natural sunlight[9]. A fundamental open question concerns the extent to which Nature might exploit such correlations[10, 11]. The study of coherent effects in biologically relevant systems has attracted increasing attention due to the observation of long-lasting oscillatory signals measured with time-resolved techniques [6, 7, 8]. This has been followed by a wave of theoretical work concentrated on these systems’ excitonic and vibrational properties[12, 13], and recently on the role of electronic coherence in the process of light absorption[14].

The nontrivial correlations within thermal light have also attracted attention for their unexpected consequences including subwavelength interference[15], ghost imaging[16] and photon-number correlations[17]. Blackbody radiation emitted by the Sun at a surface temperature of $T \simeq 5700K$ has an estimate spatial correlation length of $r_c \sim \hbar c/k_B T \sim 400nm$ [18]. Therefore photosynthetic organisms within this length-scale range should experience the spatial coherence within sunlight and other light sources. This raises the question that we address in this paper, of how they cope with, adapt to and even profit from, such correlations in the incident light.

Our findings show quantitatively that (i) the organization of the antennae complexes within a photosynthetic membrane complements the spatial correlations naturally present in sunlight; (ii) either an ordered or disordered antennae structure is favored depending on the availability of light and its metabolic needs, yielding high-efficiency photon absorption for low light-intensity environments and protection for high light-intensity environments; (iii) the macro-molecular aggregation of harvesting structures displays a high sensitivity to spatial correlations which then affects the exciton migration and subsequent charge separation at the reaction center (RC); (iv) high core-core clustering membranes yield an enhancement of the photosynthetic efficiency that is not observed for membranes with low core-core clustering; (v) the complementarity between the spatial correlations in the incident light and the evolved biomaterial structure not only enhances photon capture and efficiency, but can also guide the organization (Fig 1.(a)) and types of antennae (Fig 1.(b)) to better serve the organism’s metabolic needs. Previous work has discarded spatial correlations in the incident light as negligible and hence overlooked these five consequences.

Since our goal is to explore how spatial correlations may not only be exploited by existing photosynthetic

membranes but also help shape their evolution, we consider the simplest possible setup for a primitive photosynthetic system: sunlight (i.e. thermal light from a blackbody emitter) incident on N pigments (individual or aggregates) that can each absorb a photon and transfer the energy to neighboring molecules. Such pigments are present in all photosynthetic systems[1, 5, 19].

We focus our modeling on monochromatic polarized thermal light, though our findings generalize to multiple frequencies and polarizations. We start by considering photo-excitations arising in a time interval (τ) that is shorter than the coherence time of the light (τ_c) – however we have checked that the main findings are robust to detection times that are a factor of 100 or higher than τ_c (see Supplementary Information SI). The joint probability $P(n_1, n_2, \dots, n_N)$ that n_i photo-excitations will be registered by the i 'th molecular antenna ($i = 1, \dots, N$) is related to the generating function $G(s_1, s_2, \dots, s_N) = G(\{s_i\})$ [20] (see SI). The second-order degree of coherence of the radiation field between antennae located at \vec{r}_i and \vec{r}_j is denoted as $g_{i,j}$ and $\langle n_i \rangle$ is the average number of photo-counts at the i 'th antenna. The latter is directly connected with the mean intensity ($\langle I_i \rangle$) through the relation $\langle n_i \rangle = \alpha_i \langle I_i \rangle \tau$, where α_i is the quantum efficiency of the i 'th antenna. It is known from purple bacteria[1, 21, 22, 23], which are among the first examples of photosynthetic membranes formed on Earth, that a typical $\simeq 200$ nm wide photo-receptive harvesting vesicle will be entirely contained inside the coherence area of sunlight. The probability of detection of $n = \sum_i n_i$ photons regardless of the specific counting record of any individual antenna, is (see SI):

$$P(n) = \frac{(-1)^n}{n!} \frac{\partial^n}{\partial s^n} \{ \text{Det} [\hat{1} + \langle n \rangle s \hat{g}] \}_{s=1}^{-1} \quad (1)$$

where $\hat{1}$ and \hat{g} are the identity and the second-order degree of coherence $N \times N$ matrices respectively. For thermal radiation, the latter as registered by detectors placed at \vec{r}_i and \vec{r}_j , i.e. $g_{i,j}$, obeys the analytical expression[18, 24]

$$g_{i,j} = \frac{2J_1(u_{i,j})}{u_{i,j}} \quad (2)$$

where $J_1(z)$ is a Bessel function, $u_{i,j} = \kappa |\vec{r}_i - \vec{r}_j|$ is the effective ratio between the detectors' separation and the spatial coherence length, with κ depending on the average wavelength, the size of the source and source-detector separation. Two limiting cases illustrate the important impact of spatially correlated photons: (1) Full spatial coherence, where the area contained by the N antennae is much smaller than the coherence

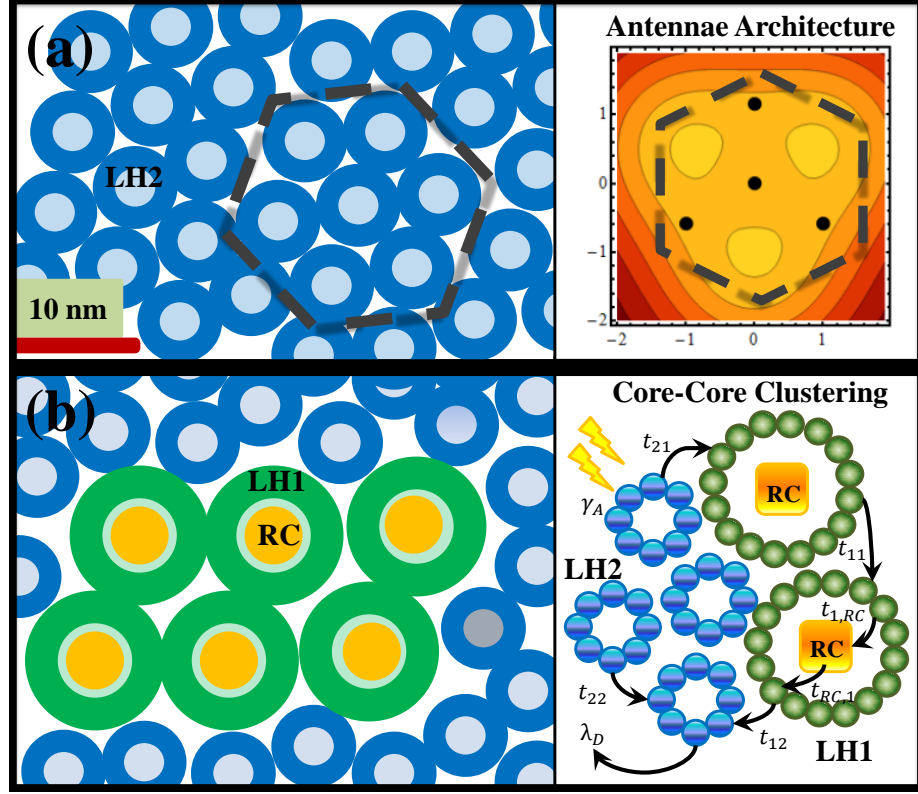


Figure 1: Typical antennae organization of low-light adapted photosynthetic purple bacteria. (a) Schematic representation of real AFM images of low-light adapted native membrane of *Rsp. photometricum* displaying LH2 hexagonal packing[27] and probability of detecting 4 photons by a configuration of five molecular antennae. The latter shows an optimal arrangement for hexagonal architecture. (b) Schematic representation of real AFM images of *Rhodobacter sphaeroides*[19] showing high core-core clustering and our theoretical model of excitation transfer and RC ionization.

area of the thermal light ($g_{i,j} = 1$ for any pair of detectors). This yields the Bose-Einstein distribution (see SI) where the average photon number $\tilde{n} = N\langle n \rangle$, and with the exciting light able to display non-classical correlations, e.g., the Hanbury-Brown-Twiss effect[18, 25, 26]. (2) No spatial coherence, i.e. $g_{i,j} = 0$ where $i \neq j$, where the distance between any two antennae is larger than the spatial coherence length of the thermal light. The resulting two-parameter distribution only reduces to the Poisson distribution in the limits $N \rightarrow \infty$ and $\langle n \rangle \rightarrow 0$ with $\tilde{n} = N\langle n \rangle = \text{constant}$.

Figure 2 shows explicitly how the incident light's spatial correlations impact the probability of photon

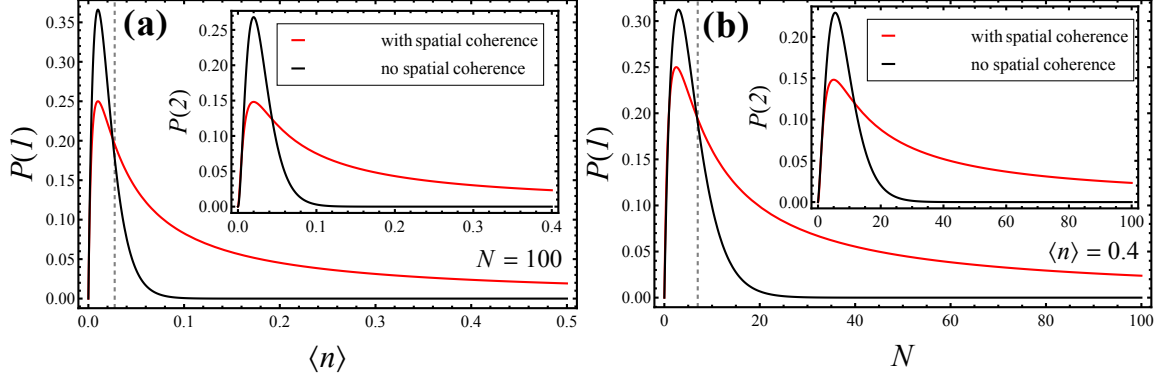


Figure 2: Effects of spatial coherence on photo-detection statistics. Probability of detection of one photon $P(1)$ as a function of (a) intensity $\langle n \rangle$ for a cluster of $N = 100$ molecular antennae, and (b) number of molecular antennae (N) for a fixed intensity ($\langle n \rangle = 0.4$). Red lines correspond to full spatial coherence, i.e. $g_{i,j} = 1$. Black lines correspond to no spatial coherence, i.e. $g_{i,j} = 0$ with $i \neq j$. Dashed lines indicate the crossing points between the full coherence and incoherence description at (a) $\langle n \rangle = 0.025$ and (b) $N = 7$. Insets show the probability for detecting photon pairs, $P(2)$.

detection by the N molecular antennae. Different light intensities are particular to the specific niche of the photosynthetic organism. For a wide range of $\langle n \rangle$ (i.e., $\langle n \rangle \geq 0.025$ in Fig. 2(a)) and for molecular antennae that are clustered within the coherence radiation area as in realistic photosynthetic membranes ($N > 7$ in Fig. 2(b)), the probabilities for 1 and 2-photon detection are consistently higher for spatially coherent light than for fully incoherent light (see Fig.S1 for multiple photons). These probabilities are fairly insensitive to fluctuations in $\langle n \rangle$ and N and hence offer robustness protection to the underlying membrane against atmospheric variations and the recurrent photo-bleaching of pigments. The fact that the probability distribution with full spatial coherence is greater than that for no spatial coherence across essentially the full range of \tilde{n} , proves that the coherence of sunlight will increase the photo-detection.

We now analyze the effect of spatial coherence on simple antennae architecture motifs from which larger membrane structures can be built. Figure 3 illustrates the photo-count statistics for a configuration of five antennae and three values of light intensity. The configuration consists of three molecular antennae in an equilateral triangle and a fourth one at the center. The probabilities of detecting $n = 1, 2$ and 3 photons are calculated as a function of the position of the fifth antennae.

The configuration of photo-detectors (Fig.3) that maximizes the underlying probability associated with a specific number of photo-detections, is remarkably similar to the honeycomb architecture found in several species of purple bacteria[21, 23, 27, 28]. The number of photons n , whose probability is maximized, is directly related to the light intensity. Importantly, for light intensity characterized by $\langle n \rangle = 0.5$, the honeycomb architecture maximizes the probability of detecting one photon (Fig. 3(a)). Interestingly, for larger light intensities, the honeycomb architecture maximizes the probability of detecting a larger number of photons. For example, for $\langle n \rangle = 1$ and $\langle n \rangle = 1.45$, the detection of two (Fig. 3(b)) and three (Fig. 3(c)) photons by a hexagonal architecture is optimal, respectively. This suggests that for a given light intensity, the organism positions antennae detectors such that the spatial coherence can better support the metabolic needs by either maximizing absorption (symmetrical architecture) or protecting the membrane from damage due to overexposure (disordered architecture). These statements are consistent with the observed chromatic adaptation of the antennae complexes to the light intensity during the growing stage[1, 23, 29]. However, our findings suggest that the photosynthetic apparatus adapts to both the incident light's intensity and correlations. By contrast, in the case of no spatial coherence, there is no preferred position for the fifth detector and hence the light offers no guiding organizational principle (see SI).

Having established the impact of light's spatial coherence on photon absorption for highly primitive geometric motifs, we examined consequent effects for actual architectures in purple bacteria (e.g. Fig.1(b) corresponding to *Rb. sphaeroides*[19]). Although we consistently observed robustness in the performance (i.e. efficiency) of prototypical architectures for arrival time traces characterized by power-law (as expected from Bose-Einstein statistics) or Poisson distributions within the biologically relevant light intensities[1] ($\approx 10\text{W/m}^2$), specific spatial correlations have a prominent impact on the dynamics of the purple bacteria's metabolic output. Our current model places consecutive absorptions within a correlation radius r . The resultant excitation diffuses until either dissipation occurs or an RC is reached. This RC might be available to produce charge separation depending on whether an average time τ_{RC} (of a few milliseconds) has elapsed after the previous charge separation in that specific RC occurred (see SI). Our model[5] successfully explains structural preferences in adaptation of purple bacteria[1, 23, 29] and incorporates excitation transfer[4] along with charge separation dynamics, which are then complemented in this study, with the absorption correlation

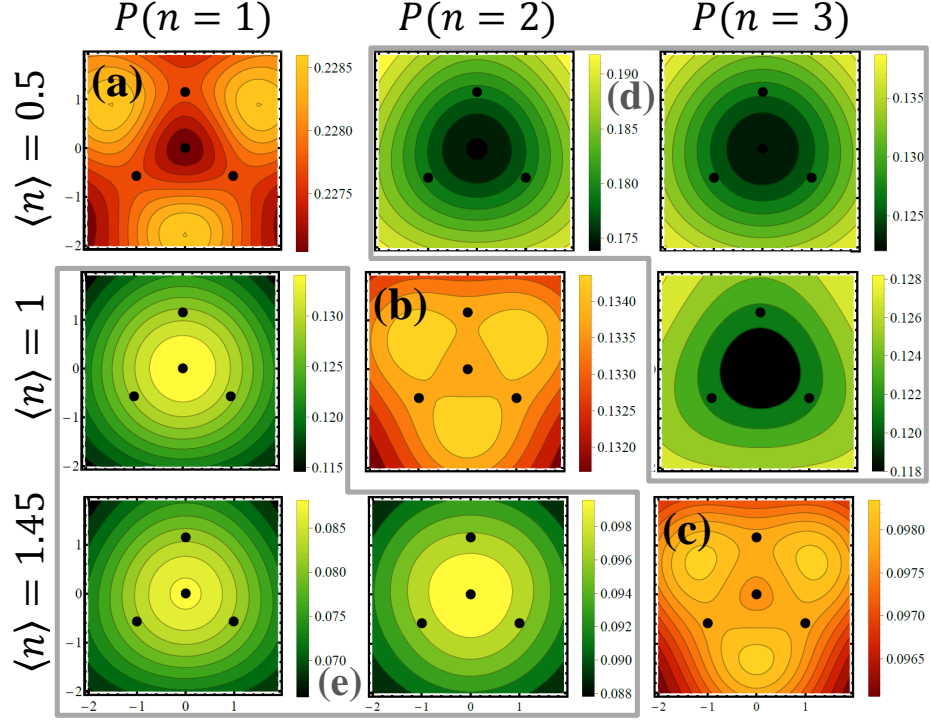


Figure 3: Numerical evaluation of the full joint probability for $N = 5$ molecular antennae. The value of $P(n)$ is plotted as a function of the position of the 5'th detector in the $x - y$ plane, with the remaining 4 antennae fixed in space (large black dots). Results are shown for spatially coherent light at low intensity (a-d), medium intensity (e-h) and high intensity (i-l). The dimensionless distance between nearest neighbor detectors is fixed to $u = 1$ (see Eq.(2)) and all distances in the $x-y$ plane are measured in terms of this inter-detector distance.

radius r .

The membrane's performance is quantified by its efficiency η , defined as the ratio of photo-excitations that produce charge separation in the RCs, to the total number of absorbed photons. Similarly, we define the relative efficiency η/η_{RA} , to compare the efficiency of correlated photons, η , and the efficiency η_{RA} for the scenario where spatial correlations are not accounted for. We study membranes which have the same number of LH1 and LH2 complexes, but differ on the specific architecture/configuration of complexes, in particular, in the RC-LH1 core-core clustering. Hence, the contrasting situations of high core-core clustering, (HCC, Fig.4(a)) and sparse low core-core clustering (LCC, fig 4(b)), differ in terms of the mean number of RC-LH1 which encircle any RC-LH1 core-complex. Figure 4(a) represents well the maximal core-core clustering that is observed in *Rsp. photometricum* for low-light intensity growth[22] with a linear core arrangement similar to *Rb. sphaeroides*[19], while Fig.4(b) resembles the vesicles grown under high-light intensity in *Rsp. photometricum*[22].

Figure 4(c) shows the striking result that HCC membranes benefit from the spatial correlations present in the incident sunlight. Our model captures a peak enhancement in the photosynthetic efficiency for membranes with HCC clustering (blue triangles), which is however absent in the LCC (red circles). Our simulations use a RC cycling time of $\tau_{RC} = 12.5\text{ms}$ consistent with experiments[30], however we find that our findings are robust for up to $\tau_{RC} = 50\text{ms}$. This novel finding suggests that the core-core clustering found in low intensity growth vesicles may profit from the spatial correlations of thermal light. Our simulations reveal that HCC presents a reduction in the number of complexes visited before charge separation takes place, when consecutive absorptions occur within radii compatible with the core clusters size. This can be understood as a benefit of placing clustered cores in the presence of the incident thermal light which is spatially bunched. Since the LH1-RC core aggregation reduces the probability of the excitation's dissipation, such a benefit could explain why several species present trends of core-core dimerization, namely *Rb. blasticus* or *Rb. sphaeroides*[19, 27], core-core clustering in *Rsp. photometricum*[22], or the self-organization in hexagonal lattices of RC-LH1 complexes in *R. rubrum*[28]. For negative spatial correlation in the incident light (i.e. opposite of natural sunlight), the peak disappears as shown in Fig.S3 of SI. The increment in efficiency shown in Fig.4(c) should not be regarded as negligible: It has been demonstrated that for these organisms, large

structural variations occur as a result of seemingly modest metabolic benefits. For example, *Rsp. acidophila* develops an expensive structural adaptation under low intensity illumination that gradually replaces LH2 by LH3 complexes which, due to a red shifted maximum, improves the transfer to the LH1 which in turn improves the membrane's efficiency by 3-4%[4].

Our results also speak to open questions about the purpose of membrane organization[19, 21], showing that it allows the system to harvest not only the light's energy, but also to profit from its spatial correlations. While other energetic and metabolic factors (e.g. complexes affinity and charge carrier diffusion) may ultimately dictate a given membrane's architecture in a given environment, our work shows for the first time that spatial correlations in sunlight potentially play a key role, and should not be ignored.

Methods: We use the general formalism of photoelectric counting statistics on molecular antennae geometries presented in Ref. 20. The limits of incoherence and coherence distribution as well as the extension to arbitrary detection times are explained in detail in the SI. Our stochastic model of the membranes excitation dynamics is presented in Ref. 5. Details are also given in the SI, together with a detailed discussion of the empirically determined parameters used as input. The validity of our detailed theoretical model is verified by its demonstrated prediction of structural preferences in purple bacteria as a function of light intensity together with the close agreement between its output and an analytical version based on coupled Master Equations (see SI Fig. S4).

Acknowledgments: A.D.M., F.R. and L.Q. acknowledge financial support from project *Quantum control of non-equilibrium hybrid systems-Part II*, UniAndes-2015. F.C.S. acknowledges support from the EU project PAPETS, the ERC Synergy grant BioQ and the DFG via the SFB TR/21.

Author Contributions: N.J., L.Q. and F.R. designed the study. P.M., A.D.M. and F.C.S. implemented the analyses and simulations. N.J., L.Q., P.M. and F.C.S. interpreted results and wrote the paper. All authors reviewed the manuscript.

Competing Interests: The authors declare that they have no competing financial interests.

Correspondence: Correspondence and requests for materials should be addressed to N.J. (email: n.johnson1@miami.edu).

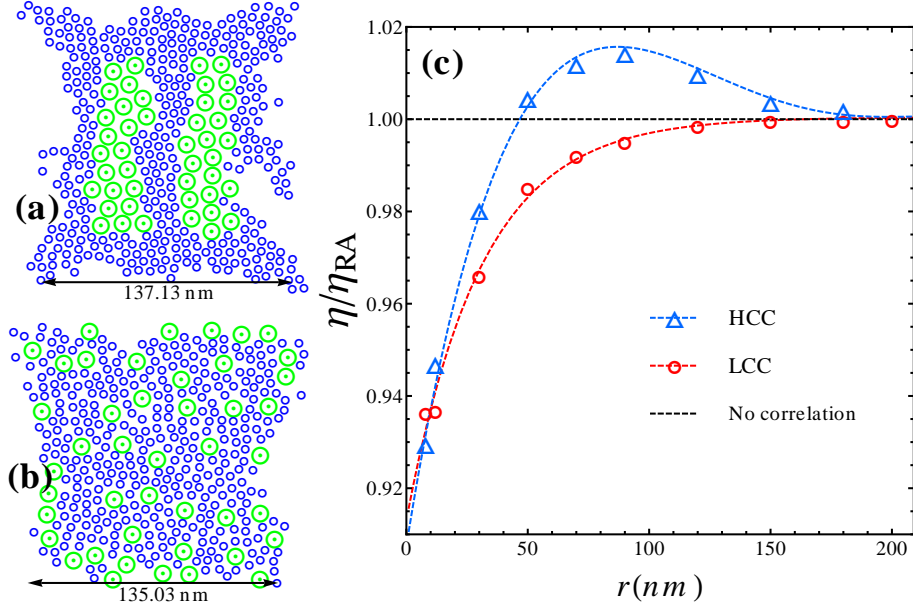


Figure 4: Methabolic implications of spatially correlated photon arrival. Architectures of the antenna complexes (a) HCC and (b) LCC. They are obtained as local minima in a large-scale Monte Carlo energy minimization, and are hence realistic as (locally stable) minimum energy structures. Blue rings represent LH2 antennae and green rings are core RC-LH1 complexes. (c) Photosynthetic relative efficiency as a function of the correlation parameter r for architectures HCC (triangles) and LCC (circles). Dashed black line illustrates the result without light correlation. Symbols represent the result from our model while lines correspond to the fitting of our simulation points. The RC closure time is $\tau_{RC} = 12.5\text{ms}$.

References

- [1] Scheuring, S. and Sturgis, J. N. Chromatic adaptation of photosynthetic membranes. *Science* **309**, 484-487 (2005).
- [2] Blankenship, R. *Molecular Mechanisms of Photosynthesis*. (Wiley-Blackwell, Tempe, 2002).
- [3] Scholes, G., Fleming, G., Olaya-Castro, A. and van Grondelle, R. Lessons from nature about solar light harvesting. *Nature Chemistry* **3**, 763-774 (2011)
- [4] Hu, X., Ritz, T., Damjanovic, A., Autenrieth, F. and Schulten, K. Photosynthetic apparatus of purple bacteria. *Quarterly Reviews of Biophysics* **35**, 1-62 (2002)
- [5] Caycedo-Soler, F., Rodriguez, F. J., Quiroga, L. and Johnson, N. F. Light-Harvesting Mechanism of Bacteria Exploits a Critical Interplay between the Dynamics of Transport and Trapping. *Phys. Rev. Lett.* **104**, 158302 (2010).
- [6] Engel, G.S. et al., Evidence for wavelike energy transfer through quantum coherence in photosynthetic systems. *Nature* **446**, 782-786 (2007).
- [7] Collini, E. et al. Coherently wired light-harvesting in photosynthetic marine algae at ambient temperature. *Nature* **463**, 644-647 (2010).
- [8] Romero, E. et al. Quantum coherence in photosynthesis for efficient solar-energy conversion. *Nature Physics* **10**, 676-682 (2014).
- [9] Ragy, S. and Adesso, G. Nature of light correlations in ghost imaging. *Scientific Reports* **2** 651; DOI:10.1038/srep00651 (2012).
- [10] Sim, N. et al., Measurement of Photon Statistics with Live Photoreceptor Cells. *Phys. Rev. Lett.* **109**, 113601 (2012).
- [11] Brumer, P. et al., Molecular response in one-photon absorption via natural thermal light vs. pulsed laser excitation. *Proceedings of the National Academy of Sciences* **109**, 48:19575-19578 (2012).

- [12] Christensson, N., Kauffmann, H. F., Pullerits, T. and Mancal, T. Origin of long-lived coherences in light-harvesting complexes. *J. Phys. Chem. B* **16**, 7449-7454 (2012).
- [13] Chin, A.W., et al. The role of non-equilibrium vibrational structures in electronic coherence and recoherence in pigment protein complexes. *Nature Physics* **9**, 113-118 (2013).
- [14] Schroeder, C. A., Caycedo-Soler, F., Huelga, S. F. and Plenio, M. B. Optical signatures of quantum delocalization over extended domains in photosynthetic membranes. *J. Phys. Chem. A* **119**, 9043-9050 (2015)
- [15] Cao, D. Z., Ge, G. J. and Wang, K. Two-photon subwavelength lithography with thermal light. *Appl. Phys. Lett.* **97**, 051105 (2010).
- [16] Zhou, Y., Simon, J., Liu, J. and Shih, Y. Third-order correlation function and ghost imaging of chaotic thermal light in the photon counting regime. *Phys. Rev. A* **81**, 043831 (2010).
- [17] Chen, H., Peng, T. and Shih, Y. 100% correlation of chaotic thermal light. *Phys. Rev. A* **88**, 023808 (2013).
- [18] Mandel, L. and Wolf, E. *Optical coherence and Quantum Optics*. (Cambridge University Press, Cambridge, 1995).
- [19] Bahatyrova, S., et al. The native architecture of a photosynthetic membrane. *Nature*, **430**, 1058-1062 (2004)
- [20] Zardecki, A. Application of the Functional Formalism to Investigation of the Photoelectric Counting Distribution. *Can. J. Phys.* **49**, 1724-1730 (1971).
- [21] Simon Scheuring, S. and Sturgis, J. N. Dynamics and Diffusion in Photosynthetic Membranes from *Rhodospirillum Photometricum*. *Biophys. J.* **91**, 3707-3717 (2006)
- [22] Scheuring, S., Rigaud, J. L. and Sturgis, J. N. Variable LH2 stoichiometry and core clustering in native membranes of *Rhodospirillum photometricum*. *EMBO J.* **23**, 4127-4133 (2004)

- [23] Scheuring, S., Goncalves, R. P., Prima, V. and Sturgis, J. N. The Photosynthetic Apparatus of *Rhodospseudomonas palustris*: Structures and Organization. *Journal of Molecular Biology*. **358**, 83-96 (2006)
- [24] Cantrell, C. D. and Fields, J. R. Effect of Spatial Coherence on the Photoelectric Counting Statistics of Gaussian Light. *Phys. Rev. A* **7**, 2063-2069 (1973).
- [25] Hanbury Brown, R. and Twiss, R. Q. Interferometry of the Intensity Fluctuations in Light. I. Basic Theory: The Correlation between Photons in Coherent Beams of Radiation. *Proc. R. Soc. A* **242**, 300-324 (1957);
- [26] Hanbury Brown, R. and Twiss, R. Q. Interferometry of the Intensity Fluctuations in Light II. An Experimental Test of the Theory for Partially Coherent Light *Proc. R. Soc. A* **243**, 291-319 (1958).
- [27] Sturgis, J. and Niedermann R. Atomic force microscopy reveals multiple patterns of antenna organization in purple bacteria: implications for energy transduction mechanisms and membrane modeling. *Photosynth Res.* **95** 269-278 (2008)
- [28] Karrasch, S., Bullough, P.A. and Ghosh, R. The 8.5Å projection map of the light-harvesting complex 1 from *Rhodospirillum rubrum* reveals a ring composed of 16 subunits. *EMBO J.* **14**, 631-638 (1995).
- [29] Adams, P. G. and Hunter, C. N. Adaptation of intracytoplasmic membranes to altered light intensity in *Rhodobacter sphaeroides*. *Biochimica et Biophysica Acta* **1817**, 1616-1627 (2012)
- [30] Milano, F., Agostiano, A., Mavelli, F., & Trotta, M. Kinetics of the quinone binding reaction at the Q_B site of reaction centers from the purple bacteria *Rhodobacter sphaeroides* reconstituted in liposomes. **2003**. *Eur. J. Biochem.* **270**, 4595-4605.